

Original Paper

Neuromedin S Increases L-type Ca^{2+} Channel Currents Through $\text{G}_{i\alpha}$ -protein and Phospholipase C-dependent Novel Protein Kinase C Delta Pathway in Adult Rat Ventricular Myocytes

Run-Xiang Chen Feng Liu Yong Li Guang-An Liu

Department of Cardiology, Suzhou Kowloon Hospital Shanghai Jiaotong University Medical School, Suzhou

Key Words

Neuromedin S (NMS) • L-type Ca^{2+} channels • Ventricular myocytes

Abstract

Neuromedin S (NMS), a peptide structurally related to NMU, has been identified in the mammalian heart tissues. However to date, any role of NMS in cardiomyocytes and the relevant mechanisms still remain unknown. In this study, we identified a novel functional role of NMS in modulating L-type Ca^{2+} channels in adult rat ventricular myocytes, in which NMU type 2 receptors (NMUR2), but not NMUR1, are endogenously expressed. We found that NMS at 0.1 μM reversibly increased I_{Ba} by ~29.7%. Intracellular infusion of GDP- β -S or a selective antibody raised against the G_i -protein blocked the stimulatory effects of NMS. The classical and novel protein kinase C (nPKC) antagonist calphostin C or chelerythrine chloride, as well as the phospholipase C (PLC) inhibitor U73122, abolished NMS responses, whereas a classical PKC antagonist Gö6976 or a PKA antagonist PKI 5-24 had no such effects. Pretreatment of cells with PKC- δ specific inhibitor rottlerin or intracellular application of a PKC- δ -derived inhibitory peptide, $\delta\text{V1-1}$, abolished NMS responses, while an inactive control peptide had no effects. In summary, NMS acting through NMUR2 increases I_{Ba} via a $\text{G}_{i\alpha}$ -protein-dependent PKC- δ pathway in rat ventricular myocytes.

Copyright © 2012 S. Karger AG, Basel

Introduction

Recently, a 36 amino acid peptide related to neuromedin U (NMU) was discovered in rat brain, named neuromedin S (NMS) owing to its high expression in the spinal cord [1]. These two peptides share the same amidated C-terminal heptapeptide and bind to the same G-protein-coupled receptors, NMU type 1 (NMUR1) and type 2 (NMUR2) receptors, with NMUR2 has a greater affinity for NMS than NMU [2]. Compared to NMU, NMS mRNA has a more limited distribution with the highest levels of expression in the hypothalamus, spleen, testis, and heart [2-4]. By activation of NMU receptors, NMS has been implicated in regulating a variety of physiological functions, including stress response, energy balance, blood pressure and heart rate modulation [5-6]. For example, in cardiovascular system, NMS has been reported to elicit a rapid and sustained increase in blood pressure [7]. In addition, rat NMS produced a significant increase in heart rate in the chronically instrumented rat model [8]. However to date, whether NMS would directly affect the function of cardiac myocytes as well as the relevant mechanisms remain still unknown.

L-type Ca^{2+} channels are voltage-dependent channels that open in response to membrane depolarization to allow the entry of Ca^{2+} into the cell. Ca^{2+} entry through L-type Ca^{2+} channels is critical in the control of cardiac function and contributes to physiological frequency regulation in the sinus node [9-12]. Furthermore, L-type Ca^{2+} channel is an important parameter for the duration of the plateau phase of the action potential and refractoriness, and plays a fundamental role in the process of Ca^{2+} release from the sarcoplasmic reticulum, raising free intracellular Ca^{2+} concentration ($[\text{Ca}^{2+}]_i$) and allowing cell contraction [13]. Moreover, it is clear that $[\text{Ca}^{2+}]_i$ serves as an important second messenger in the regulation of gene expression in life-threatening cardiac diseases [14]. Nonetheless, little information is available for the mechanism involved in the effect of NMS on cardiac L-type Ca^{2+} channels.

Therefore, the present study was undertaken to elucidate the signaling pathways implicated in cardiac L-type Ca^{2+} channel modulation by NMS in adult rat ventricular myocytes, in which NMUR2, but not NMUR1, were endogenously expressed. Based on pharmacological manipulation of NMS-induced I_{Ba} increase, we reported that NMS increased I_{Ba} via a $\text{G}_i\alpha$ -protein-dependent protein kinase C delta (PKC- δ) pathway.

Materials and Methods

Preparation of ventricle myocytes

All animal care and handling conformed to the *Guide for Care and Use of Laboratory Animals* published by the US National Institutes of Health, and the study was approved by the local institutional ethical committee. Ventricle myocytes were dissociated enzymatically by a modified method described previously [15-17]. Briefly, Sprague-Dawley rats (male, 200-300 g) were injected intraperitoneally with 1000 IU heparin and euthanized in a CO_2 chamber. The heart was quickly removed and transferred to an ice-cold Tyrode's solution. The aorta was cannulated and the heart was mounted on a Langendorff apparatus. The heart was perfused with prewarmed (at 37°C) and oxygenated Tyrode's solution containing protease type XIV (Sigma) and collagenase type I (Sigma) for 10 min until the heart was flaccid. The ventricles were dissected out, cut into small pieces, and gently stirred in the Tyrode's solution. Isolated cells were filtered and maintained in an oxygenated KB solution on ice. Only the cells with a rod shape and clear cross striation were used for experiments.

Reverse transcription-PCR (RT-PCR)

Total RNA was extracted from rat ventricle myocytes using the RNeasy kit (QIAGEN). Reverse transcription was carried out with SuperScriptTM II (Invitrogen). Reactions without reverse transcriptase were carried out in all RT-PCRs to exclude contamination. The sequences of the primers employed in this study are summarized in Table 1. The PCR protocol includes a denaturation step at 95°C for 2 min, and the denaturation, annealing, and elongation cycle was carried out at 94°C for 30 sec, at 65°C (NMUR1 and NMUR2) for 20 sec, and at 72°C for 1 min. PCR was carried out for 32 cycles (NMUR1 and NMUR2). PCR

Table 1. Primers used for RT-PCR analysis of NMUR1, NMUR2, and GAPDH.

| Gene | Primers for RT-PCR | Accession number (genbank) | Predicted size (bp) |
|-------|---|----------------------------|---------------------|
| NMUR1 | 5'-CTGCTCATTGGGCTGCGGCT-3' 5'-AGGCTGTAGAGCACCGG GTTGG-3' | NM_010341 | 262 |
| NMUR2 | 5'-ACCCAACCTTACCACCGTCCCTG-3' 5'-AGGCTAAACCCACCCATCATGA-3' | NM_153079 | 257 |

analysis was repeated at least twice with the same samples to confirm reproducibility of the results.

Western blot

Western blot analysis was performed following the procedure described by previous reports [18–20]. For antibody detection, after incubated with 5% non-fat milk in TBST for 1 h at room temperature, membranes were then incubated with diluted primary antibody goat anti-rat NMUR1 (Santa Cruz, 1:500) or NMUR2 (Santa Cruz, 1:500) and incubated at 4 °C overnight. After 5 washes with TBST, membranes were incubated for 2 h with diluted 5000-fold donkey anti-goat secondary antibody (Sigma, USA). After 5 washes, the specific binding of the primary antibody was detected with SuperSignal Ultra chemiluminescent substrate (Pierce).

Electrophysiology recording

A small aliquot of cell suspension was placed in an open perfusion chamber mounted on the stage of an inverted microscope. Myocytes were allowed to settle down to the bottom of the chamber. Only quiescent rod-shaped cells with clear striations were used. The whole-cell patch clamp experiments for recording cardiac myocytes were performed at room temperature (20–22°C). Electrodes were pulled from borosilicate glass microcapillary tubes (World Precision Instruments). They had resistances from 2 to 3 MΩ when filled with internal solution. We made recordings using a MultiClamp 700B amplifier (Molecular Devices) and controlled voltage commands and digitization of membrane currents using a Digidata 1440A interfaced with Clampex 10.2 of the pClamp software package (Molecular Devices), running on a personal computer. Currents were low-pass filtered at 2–5 kHz. Series resistance (R_s) and capacitance (C_m) values were taken directly from readings of the amplifier after electronic subtraction of the capacitive transients. Series resistance was compensated to the maximum extent possible (at least 70%). Current traces were corrected for linear capacitive leak with online P/6 trace subtraction.

Reagents and solutions

All drugs were obtained from Sigma (USA), unless otherwise indicated. NMS, GDP-β-S, QEHA, PKI 5-24, δV1-1 (PKC-δ inhibitor, amino acids 8–17 [SFNSYELGSL]), and the control scramble peptide were prepared in distilled deionized water. Stock solutions of U73122, U73343, chelerythrine chloride, rottlerin, Gö6976 and calphostin C were prepared in dimethyl sulfoxide (DMSO). The concentration of DMSO in the bath solution is expected to be less than 0.01%, and had no functional effects on L-type Ca^{2+} channel currents (not shown). For L-type Ca^{2+} channel current recordings, the external solution contained (in mM): tetraethylammonium chloride (TEA-Cl) 140, BaCl_2 2, MgCl_2 0.5, glucose 5.5, CsCl 5, and HEPES 10, pH 7.35, with TEA-OH. The pipette solution contained (in mM): CsCl 110, EGTA 10, ATP-Mg 4, GTP-Na 0.3, HEPES 25, Tris-phosphocreatine 10, pH 7.3 with CsOH, 290 mOsm. For Na^+ current recordings, the pipette solution contained the following (in mM): CsCl 120, CaCl_2 1, MgCl_2 5, Na_2ATP 5, EGTA 11, HEPES 10 (pH 7.3 with CsOH). The bath solution contained (in mmol/L): NaCl 65, CsCl 70, CaCl_2 1, CdCl_2 0.05, glucose 10, HEPES 10 (pH 7.4 with CsOH). The Tyrode's solution was composed of the following (in mM): NaCl 150, KCl 5.4, MgCl_2 2.0, HEPES 10, glucose 11. pH was adjusted with NaOH to 7.4. The KB solution was composed of the following (in mM): KOH 70, KCl 40, L-glutamic acid 50, taurine 20, KH_2PO_4 20, MgCl_2 3, HEPES 10, EGTA 0.5, glucose 10 (pH 7.35–7.40 with KOH).

Data analysis

All data are expressed as mean±S.E.M., and GraphPad Prism 5.0 was used for electrophysiological data plotting. Student's *t*-tests or one-way ANOVA were used to compare the different values, and were

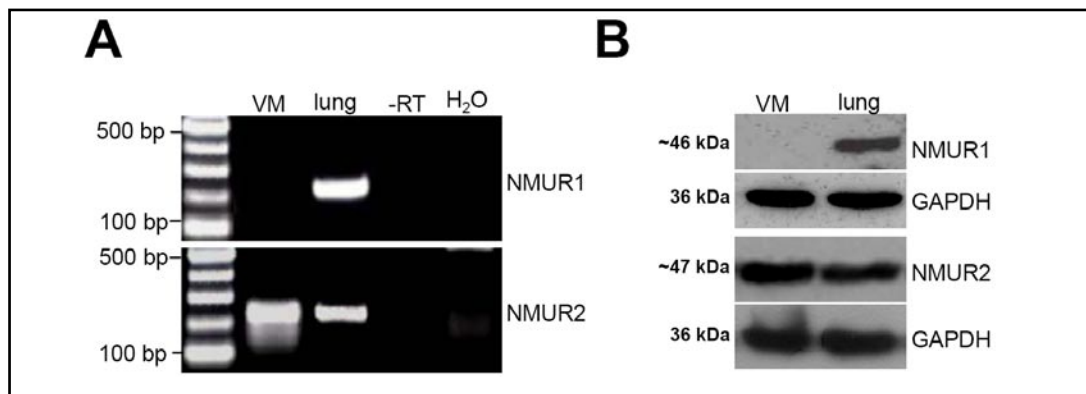


Fig. 1. Expression of NMU receptors in adult rat ventricular myocytes. A, detection of NMUR1 (upper panel) and NMUR2 (lower panel) mRNA in rat ventricular myocytes. Total RNA from rat lung was used as a positive control for both NMUR1 and NMUR2. Minus RT (-RT) indicates RT-PCR reaction without the addition of RT. B, western blot analysis of NMUR2 (~47 kDa) protein expression in rat ventricular myocytes. Rat lung expressing both NMUR1 (~46 kDa) and NMUR2 (~47 kDa) is used as positive control. GAPDH (36 kDa) was used as loading control.

considered significant at 0.05 or lower. Concentration-response curves were fitted by sigmoidal Hill equation $I/I_{\text{control}} = 1/(1 + 10^{(\log IC_{50} - X)n_h})$, where X is the decadic logarithm of the concentration used, IC_{50} is the concentration at which the half-maximum effect occurs, and n_h is the Hill coefficient. Activation data were fitted by: $G/G_{\text{max}} = F_{\text{low}} / \{1 + \exp((V_{1/2, \text{low}} - V)/k_{\text{low}})\} + (1 - F_{\text{low}}) / \{1 + \exp((V_{1/2, \text{high}} - V)/k_{\text{high}})\}$, where $V_{1/2, \text{act}}$ is the potential for half-activation calculated from dual Boltzmann functions when $G = 0.5G_{\text{max}}$. Steady-state inactivation data were fitted by a Boltzmann function of the form: $I/I_{\text{max}} = (A_1 - A_2) / \{1 + \exp((V - V_{1/2, \text{inact}})/k_{\text{inact}})\} + A_2$, where I is the test-pulse current, I_{max} is the normalization current, A_1 is initial current amplitude, A_2 is final current amplitude, V is the membrane potential of the conditioning pulse, $V_{1/2}$ is the potential for half-inactivation, and k is the slope factor.

Results

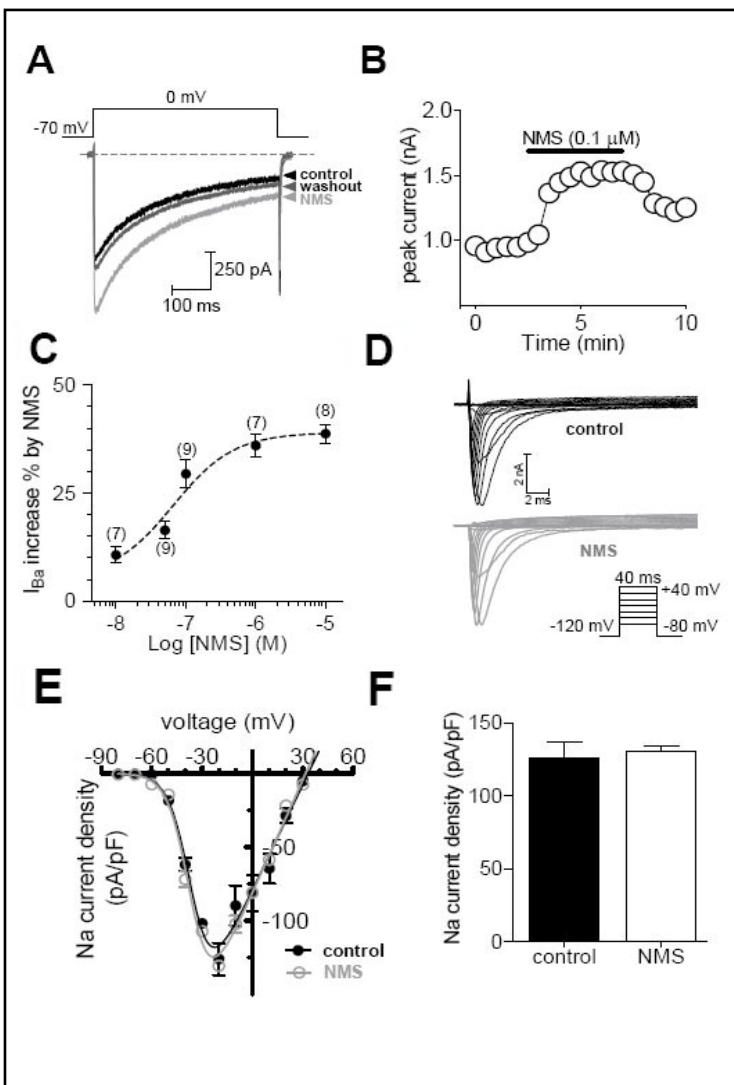
Expression of NMU receptors in adult rat ventricular myocytes

To determine whether NMU receptors were endogenously expressed in rat ventricular myocytes, we characterized the mRNA and protein expression by RT-PCR and western blot, respectively. RT-PCR analysis demonstrated that NMUR2 mRNA (predicted size of specific transcripts were 262 bp) were expressed in adult rat ventricular myocytes, whereas NMUR1 mRNA could not be detected (Fig. 1A). As positive controls, NMUR1 transcripts (predicted size of 257 bp) isolated from rat lung could be clearly amplified (Fig. 1A). The negative controls performed with water or without reverse transcriptase added to the reaction yielded no detectable band. Subsequently, we investigated the protein expression of NMU receptors in rat ventricular myocytes. Western blot analysis of protein lysates using anti-NMUR2 antibody revealed that NMUR2 was expressed at the predicted size of ~47 kDa while NMUR1 was not detected by anti-NMUR1 antibody (Fig. 1B). No band was found with goat serum (not shown). As a positive control, rat lung known to express NMUR1 showed a prominent band of ~46 kDa (Fig. 1B). GAPDH (36 kDa) was used as the loading control.

NMS dose-dependently increases I_{Ba} in adult rat ventricular myocytes

To test the regulation of NMS on L-type Ca^{2+} channel currents, we recorded barium currents (I_{Ba}) from adult rat ventricular myocytes with a holding potential of -70 mV, using an external solution containing 2 mM Ba^{2+} at room temperatures, to avoid Ca^{2+} -dependent inactivation of Ca^{2+} channels. Bath application of 0.1 μM NMS increased the basal amplitude

Fig. 2. NMS dose-dependently increased I_{Ba} . A, exemplary traces of I_{Ba} under control conditions, during exposure to 0.1 μM NMS, and washout. B, time course of changes in amplitude showed the effects of 0.1 μM NMS on I_{Ba} in adult rat ventricular myocytes. C, Dose-response curve for the stimulatory effect of NMS on I_{Ba} . The line represents the best fit of the data points to the sigmoidal Hill equation (see *Methods and Materials*). I_{Ba} were elicited by a 400 ms-long depolarizing step pulse from the holding potential of -70 mV to 0 mV. Number of cells tested at each concentration of NMS is indicated in brackets. D-E, exemplary current traces (D) and current-voltage (I-V) plot of current density (E) of Na^+ current versus test voltage recorded before ($n=9$) and after ($n=9$) 0.1 μM NMS. I-V curves were obtained from a holding potential of -120 mV, 40 ms depolarizing pulses to different membrane potentials (10 mV increments from -80 mV to +40 mV). F, summary data showed that at -20 mV 0.1 μM NMS had no effects on the peak current density of Na^+ channel currents ($n=9$).



of I_{Ba} in rat ventricular myocytes by $29.7 \pm 3.6\%$ ($n=9$, Fig. 2A). Upon washout of NMS, the amplitude of I_{Ba} partially returned within 5 min (Fig. 2B). Using the magnitude of the effect that NMS has on currents elicited by depolarization to 0 mV, it is clear that NMS increased I_{Ba} in a concentration-dependent manner (Fig. 2C). The relationship between the concentration of NMS used and the degree of increase observed is described by a logistic equation where the concentration of NMS producing half-maximal inhibition (IC_{50}) is 0.08 μM , the apparent Hill coefficient is 0.91, and the maximal stimulatory effect is $37.6 \pm 2.2\%$ ($n=8$, Fig. 2C).

Besides L-type Ca^{2+} channel currents, we also examined whether NMS affected the voltage-gated Na^+ channel currents in rat ventricular myocytes. Our results showed that application of 0.1 μM NMS failed to affect Na^+ current density at each voltage (Fig. 2D and E). As shown in Fig. 2E, the current-voltage (I-V) curves were not shifted, and at -20 mV the peak current densities were not significantly different in the presence (130.8 ± 8.7 pA/pF) or absence (126.1 ± 11.2 pA/pF) of NMS ($n=9$, Fig. 2F).

NMS rightward shifts steady-state inactivation curve

As a dose-dependent increase in the peak current density of I_{Ba} was evident, we next determined whether the biophysical properties of I_{Ba} were affected by NMS. The current-voltage (I-V) curves showed that 0.1 μM NMS significantly increased I_{Ba} at each tested voltage,

Fig. 3. NMS rightward shifted the steady-state inactivation curve. A-B, exemplary traces (A) and pooled data (B) showed the effects of $0.1 \mu\text{M}$ NMS on I-V curve. I-V curves were obtained from a holding potential of -70 mV , 400 ms depolarizing pulses to different membrane potentials (10 mV increments from -40 mV to $+60 \text{ mV}$). C, the steady-state activation of L-type Ca^{2+} channels is not altered by NMS application. Tail currents were elicited by repolarization to -70 mV after 40 ms test pulses from -50 to $+50 \text{ mV}$ in increments of 10 mV . D, NMS ($0.1 \mu\text{M}$) shifted steady-state inactivation curve of L-type Ca^{2+} channels to depolarizing direction. I_{Ba} evoked by 100 ms test pulse to 0 mV after the 3 s conditioning pulses ranging from -70 to 0 mV with 10 mV increments.

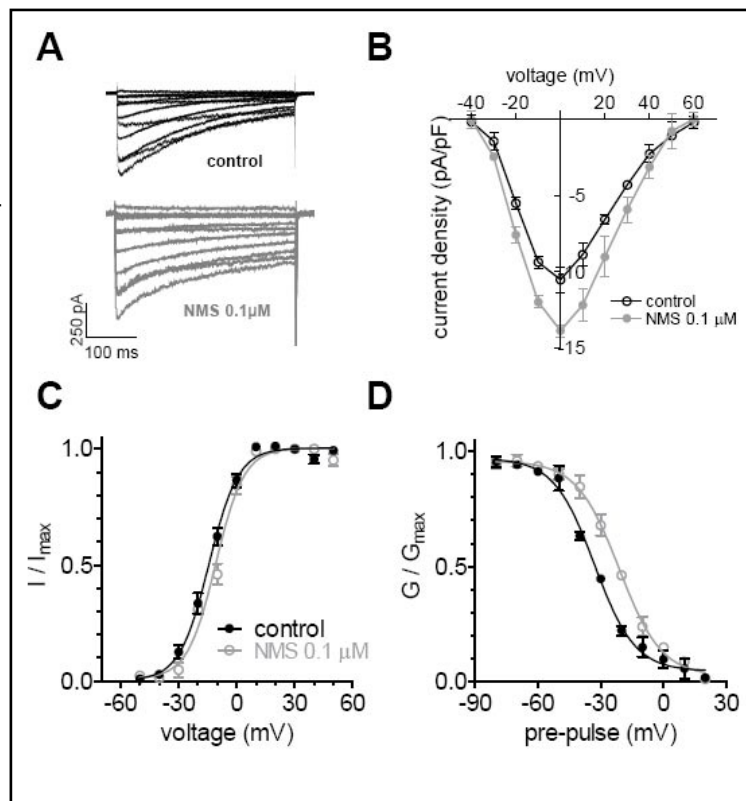
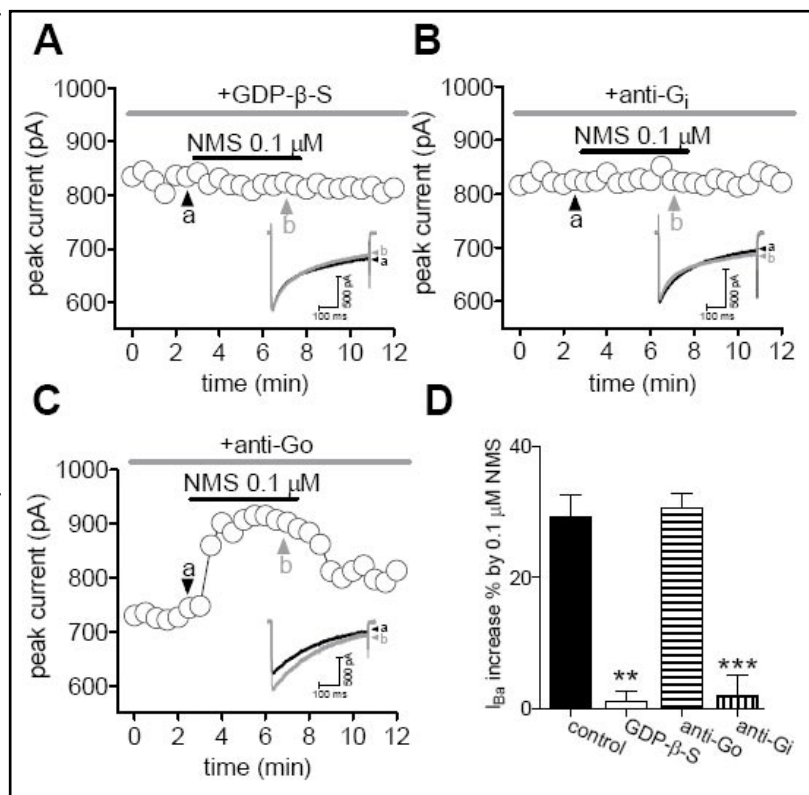
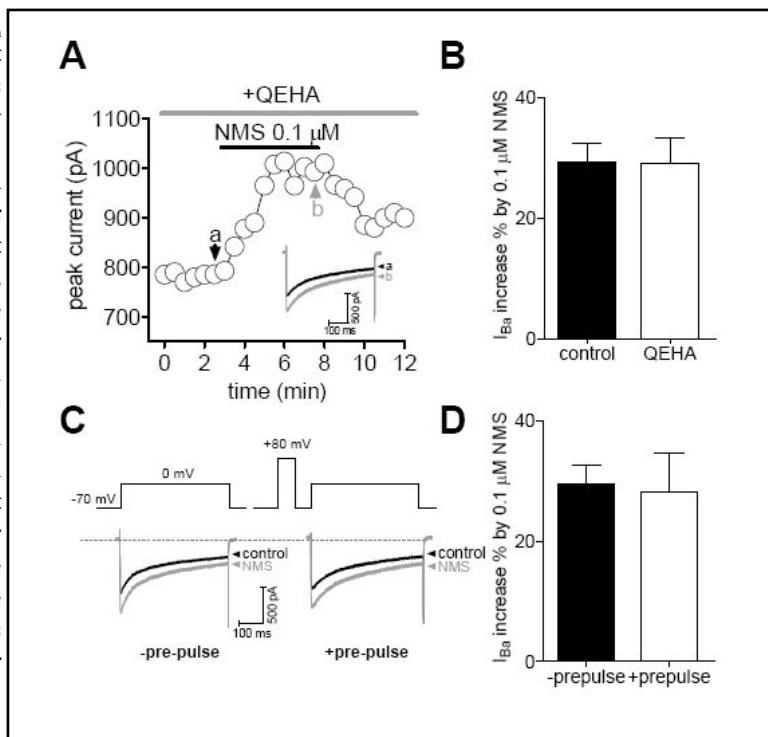


Fig. 4. Involvement of G_i -proteins in NMUR2-mediated I_{Ba} increase. A-C, time courses showed the effects of NMS ($0.1 \mu\text{M}$) on I_{Ba} in the presence of GDP- β -S (A), anti- G_i (B), and anti-Go (C), respectively. Insets showed exemplary current traces indicated in panel A through C. Alphabets on plot indicate which points were used for sample traces. D, pooled data showed the effects of dialyzing of GDP- β -S (1 mM), anti- G_i ($1:100$ dilution), or anti-Go ($1:100$ dilution) on NMS-induced I_{Ba} increase. $**p < 0.01$ vs. control, $***p < 0.001$ vs. control.



and at 0 mV the peak current density increased from $10.6 \pm 1.7 \text{ pA/pF}$ to $13.8 \pm 1.9 \text{ pA/pF}$ ($n=9$, Fig. 3A and B). We next analyzed the voltage-dependence of activation and inactivation

Fig. 5. NMS-mediated I_{Ba} increase via $G_{\beta\gamma}$ -independent pathway. A-B, time courses (A) and pooled data (B) show the effects of NMS at 0.1 μM on I_{Ba} in the presence of QEHA peptides (200 μM). *Insets* showed exemplary current traces indicated in panel A. Alphabets on plot indicate which points were used for sample traces. C-D, I_{Ba} evoked by depolarizing steps to 0 mV, from a holding potential of -70 mV, preceded by a prepulse to +80 mV. Note that NMS (0.1 μM) induced similar I_{Ba} increase in the presence or absence of prepulse depolarization. Similar results were observed in six other ventricular myocytes.



potentials (Fig. 3C and D) and observed a slight but statistically insignificant shift of 1.5 mV of the activation potential ($V_{1/2}$ from -9.9 ± 2.7 to -11.4 ± 2.2 mV and k value from 13.8 ± 1.8 to 15.1 ± 1.3 , Fig. 3C; $n=9$). In contrast, NMS at 0.1 μM significantly shifted the steady-state inactivation curve in the depolarizing direction by 8.6 mV ($V_{1/2}$ from -31.2 ± 2.6 to -22.6 ± 3.9 mV and k value from 14.7 ± 2.1 to 15.2 ± 3.6 , Fig. 3D; $n=9$), which suggest that the increase in I_{Ba} observed upon application of NMS in rat ventricular myocytes could be due to a decreased proportion of channels remaining in the inactivated state.

NMUR2-mediated I_{Ba} increase requires $G_{\beta\gamma}$ -protein

Previous reports have shown that NMUR2 was $G_{i/o}$ -protein coupled [6, 19]. To examine whether heterotrimeric G-proteins are involved in NMUR2-mediated I_{Ba} response, we dialyzed cells with guanosine-5'-O-(2-thiodiphosphate) (GDP- β -S, 1 mM), a non-hydrolysable GDP analog, and found that intracellular application of GDP- β -S completely abolished the increase of I_{Ba} induced by 0.1 μM NMS (increase% = 2.7 ± 1.6 , $n=9$, Fig. 4A and D), indicating that G-protein activation was required for NMS action. We further determined which isoform of G-protein α subunit (G_{α}) was involved in this increase. An antibody that specifically binds $G_{\beta\gamma}$, but not G_{α} subunit, was used to determine the subtype of $G_{i/o}$ involved in the NMS-induced response. Dialyzed cells with this antibody abolished the increase of NMS on I_{Ba} (increase% = 3.1 ± 1.9 , $n=8$, Fig. 4B and D) without significantly altering the current amplitude in the absence of agonist. The boiled $G_{\beta\gamma}$ -specific antibody (increase% = 30.1 ± 3.5 , $n=5$, not shown) as well as a G_{α} -specific antibody (increase% = 31.9 ± 2.7 , $n=8$, Fig. 4C and D) had no such effect. These results suggested that a $G_{\beta\gamma}$, but not G_{α} -like protein, was involved in the NMS-induced I_{Ba} increase.

$G_{\beta\gamma}$ was not involved in NMUR2-mediated I_{Ba} increase

We next determined whether the $\beta\gamma$ subunits of G_i was involved in the NMS-mediated response. QEHA (200 μM), a synthetic peptide, which competitively binds $G_{\beta\gamma}$ and blocks $G_{\beta\gamma}$ -mediated signaling [20, 21], was introduced into the recording pipette (Fig. 5A). We found that intracellular application of QEHA did not affect the stimulatory effect of NMS on I_{Ba}

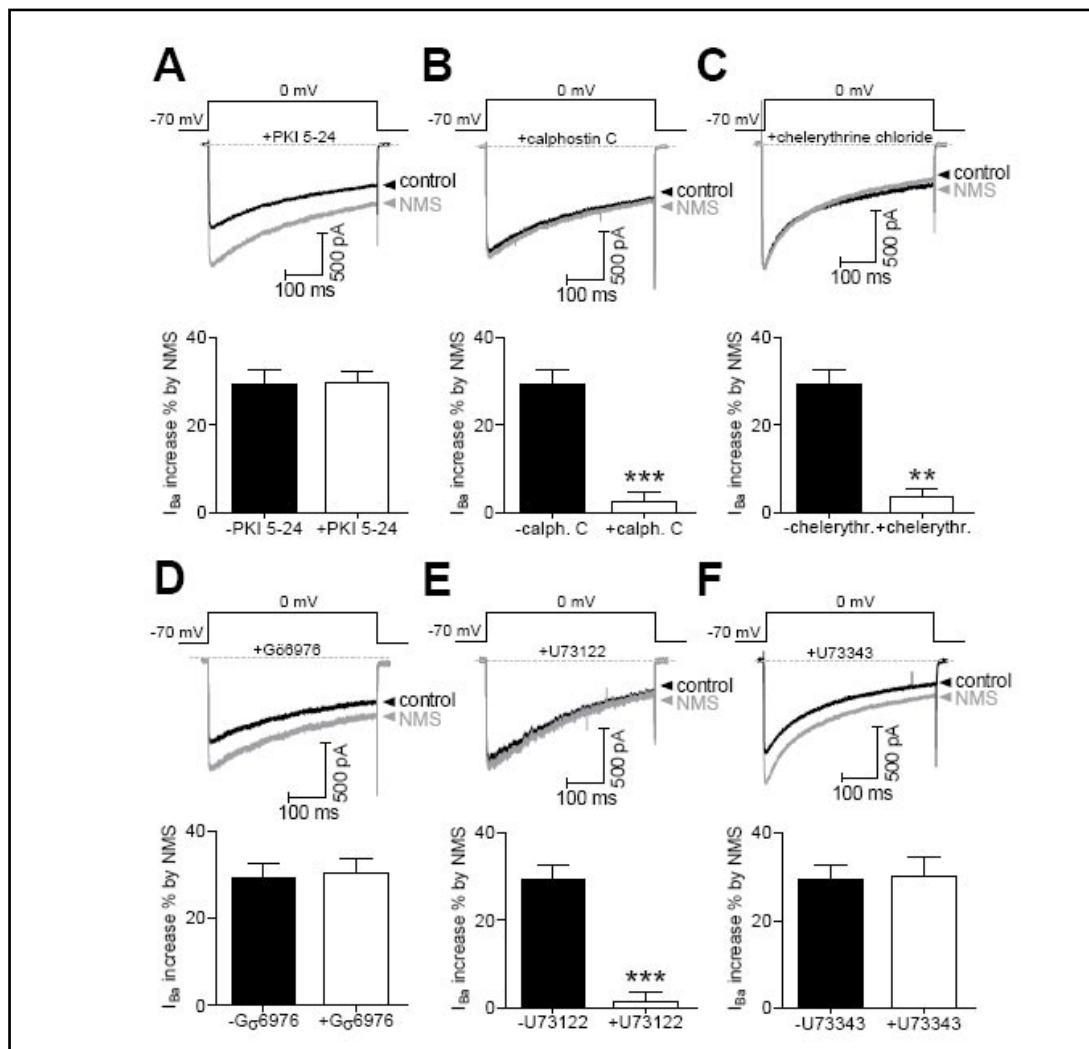


Fig. 6. NMS-induced I_{Ba} increase involves novel PKC. A-F, exemplary traces (upper panel) and pooled data (lower panel) show the increase of I_{Ba} by NMS (0.1 μM) in the presence of PKI 5-24 (1 μM , intracellular applied, A), calphostin C (50 nM, B), chelerythrine chloride (1 μM , C), Gö6976 (1 μM , D), U73122 (2 μM , E), and U73343 (2 μM , F), ** P <0.01 vs. control, *** P <0.001 vs. control.

(increase%=28.6 \pm 4.2, n =8, Fig. 5A and B), which suggested that $G_i\alpha$ -protein, but not its $G_{\beta\gamma}$, was necessary for the NMS-induced I_{Ba} increase. As a complementary test of our hypothesis, we also utilized a depolarizing prepulse to disrupt any potential $G_{\beta\gamma}$ and the L-type Ca^{2+} channel interaction. No such voltage-dependent facilitation was observed in the absence or presence of NMS (Fig. 5C). The amplitudes of I_{Ba} evoked with and without depolarizing prepulse were measured in the absence and presence of NMS. We found that NMS (0.1 μM) induced similar I_{Ba} increase in the presence (increase%=29.6 \pm 3.9 with prepulse, n =11, Fig. 5D) or absence of prepulse depolarization (29.7 \pm 3.6%, n =9, Fig. 5D). These results strongly suggested increase of I_{Ba} by NMS was not through the direct interaction of $G_{\beta\gamma}$ subunits with L-type Ca^{2+} channels in rat ventricular myocytes.

PKC- δ was involved in NMUR2-mediated I_{Ba} increase

Since activation of NMUR2 by NMS appeared to increase I_{Ba} via $G_i\alpha$ -protein, we further investigated the downstream intracellular signaling molecules. Involvement of protein kinase A (PKA) in NMS-induced I_{Ba} increase was first determined. We dialyzed the cells with a pipette

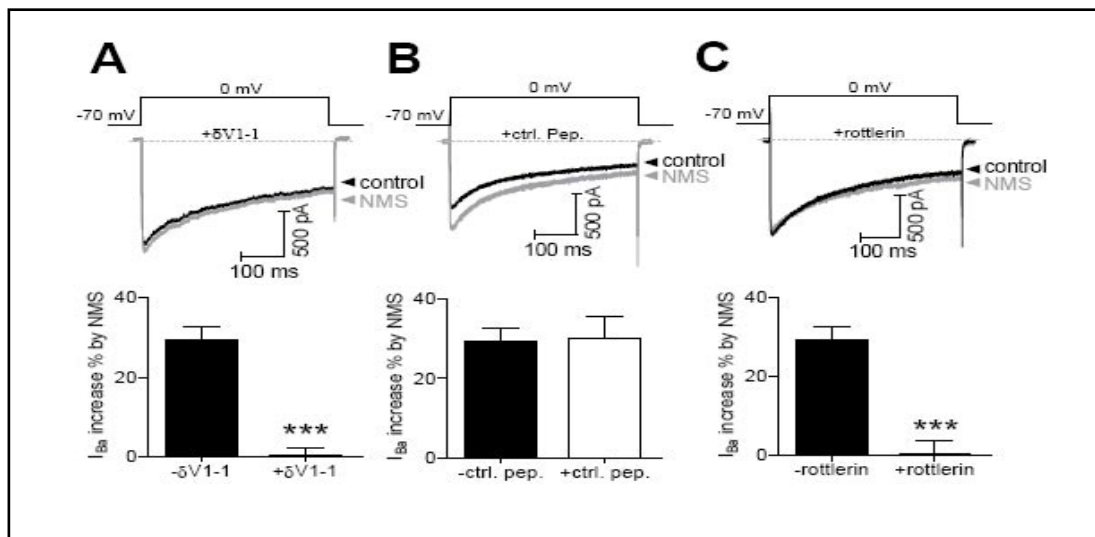
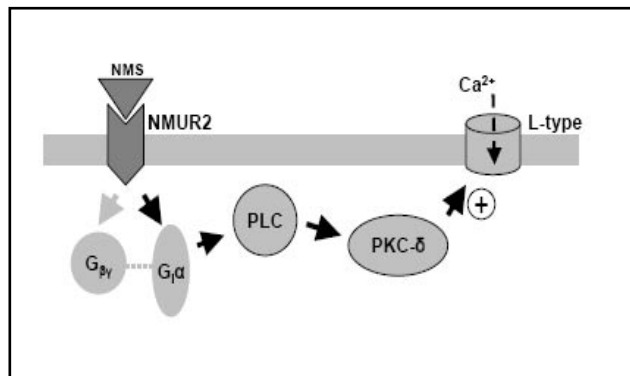


Fig. 7. PKC- δ was involved in NMS-induced I_{Ba} increase. A-C, exemplary traces (*upper panel*) and pooled data (*lower panel*) show the increase of I_{Ba} by NMS (0.1 μM) in the presence of rottlerin (1 μM , intracellular applied, A), $\delta\text{V1-1}$ (1 μM , intracellular applied, B), and the control scramble peptide (1 μM , intracellular applied, C), *** $P < 0.001$ vs. control.

Fig. 8. Model for NMUR2-mediated I_{Ba} increase in adult rat ventricular myocytes. NMS acts through NMUR2 to activate $G_{\text{q}}\alpha$ -proteins and stimulate PLC. Activation of PLC stimulates PKC- δ , which in turn stimulates the L-type Ca^{2+} channels. The direct interaction between $G_{\text{q}}\alpha$ and L-type Ca^{2+} channels is not necessary for NMUR2-mediated I_{Ba} increase. Whether PKC- δ directly phosphorylates the channel or acts on an intermediate protein remains further determined.



solution containing the PKA inhibitor, PKI 5-24, and found that that adding PKI 5-24 (1 μM) to the recording pipette solution had no effects on NMS-induced I_{Ba} increase in rat ventricular myocytes (increase% = 30.5 ± 2.1 , $n = 9$, Fig. 6A), indicating that NMS-induced I_{Ba} increase in rat ventricular myocytes was PKA-independent. As it has been reported that L-type Ca^{2+} channels can be regulated by the PKC [22], we investigated whether the stimulatory effects of NMS were PKC-dependent. Pretreatment of the cells with calphostin C (50 nM), a classical and novel PKC antagonist, abolished NMS-induced I_{Ba} increase (increase% = 2.2 ± 2.7 , $n = 9$, Fig. 6B). Similar results were obtained with another classical and novel PKC antagonist chelerythrine chloride (increase% = 2.7 ± 0.9 , $n = 9$, Fig. 6C). However, pre-incubation of the cells with the classical PKC antagonist Gö6976 (1 μM) elicited no such effects (increase% = 31.1 ± 4.2 , $n = 8$, Fig. 6D). These results together suggest that a novel PKC (nPKC) pathway might be involved in NMS-induced I_{Ba} increase.

It has been reported that $G_{\text{q}}\alpha$ -protein activation can lead to novel PKC activation via phospholipase C (PLC) [18]. Therefore, we tested the hypothesis that PLC was necessary for NMS-induced I_{Ba} increase. Indeed, the NMS-induced incremental effect of I_{Ba} was abolished by the PLC inhibitor U73122 (3 μM) (increase% = 2.7 ± 3.9 , $n = 7$, Fig. 6E). Since U73122 has been reported to have nonspecific effects on various cellular events [18], we also tested

the effects of a structurally related but inactive analogue, U73343 [18], U73343 (2 μM) had no effect on NMS-induced I_{Ba} increase (increase% = 31.6 ± 3.9 , $n=7$, Fig. 6F). In astrocytes and cardiomyocytes, PLC positively modulated the phosphorylation of novel PKC δ (PKC- δ) [23-25]. We next determine the involvement of PKC- δ in NMS-induced I_{Ba} increase. Intracellular application of a PKC- δ specific inhibitor peptide, $\delta\text{V1-1}$ (1 μM), completely abolished the NMUR2-mediated I_{Ba} increase (increase% = 0.9 ± 1.1 , $n=8$, Fig. 7A). In contrast, in cells dialyzed with an inactive PKC- δ control scramble peptide (1 μM), the NMS-induced increase of I_{Ba} was not significantly affected (increase% = 31.3 ± 2.1 , $n=7$, Fig. 7B). Similar results were obtained with another PKC- δ inhibitor rottlerin. As shown in Fig. 7C, pretreatment of cells with rottlerin (1 μM) abolished NMS-induced I_{Ba} increase (increase% = 1.7 ± 2.1 , $n=7$, Fig. 7C). These results together indicated that NMUR2-mediated I_{Ba} increase was via a PLC-dependent PKC- δ pathway.

Discussion

Neuromedin S (NMS) and its receptors are widely expressed in brain and peripheral tissues, and possess a wide spectrum of functions [2, 6]. However, the roles of NMS in the heart remain elusive. In the present study, we first demonstrated that NMS plays a novel role in modulating L-type Ca^{2+} channels in adult rat ventricular myocytes, whereas NMUR2, but not NMUR1, are endogenously expressed. Based on pharmacological manipulation of NMS-induced I_{Ba} increase, we propose that this response is coupled to a $\text{G}_i\alpha$ -protein-dependent PKC- δ pathway, which has been depicted in Fig. 8.

Predominant studies have shown that NMUR1 was more abundant in peripheral tissues, whereas NMUR2 was located more centrally [6]. However, NMUR2 located in mouse hippocampus was also reported [26]. In addition, we show in this study that NMUR2 was expressed in adult rat ventricular myocytes, whereas NMUR1 expression could not be detected. These receptor distribution patterns have started to allow the assignment of particular physiological roles of NMS and its receptors in mammals [6, 20, 26]. By using genetic model, previous studies have shown that activation of NMUR1 inhibited L-type Ca^{2+} channel currents in mouse hippocampal neurons [26]. Interestingly, in the present study, NMS significantly increased I_{Ba} through L-type Ca^{2+} channels in adult rat ventricular myocytes. The different results are not contradictory to each other, rather this may imply a distinct regulation of NMS on L-type Ca^{2+} channels via distinct receptors: as NMUR1 expresses exclusively in mouse hippocampus, instead NMUR2 in rat ventricular myocytes. In addition, there are molecular and pharmacological differences between sensory neurons and cardiovascular tissue in the L-type Ca^{2+} channels. In neuronal cells, the predominant pore-forming $\alpha 1$ -subunit is Cav1.3, whereas in cardiac muscle cells, the principal $\alpha 1$ -subunit is Cav1.2 [27, 28].

It has been previously suggested that $\text{G}_{i/o}\alpha$ could interact directly with Ca^{2+} channels [18, 29]. However, such a mechanism is not likely in our system because we observed that inhibition of PLC or novel PKC completely abolished the effect of NMS on I_{Ba} . We also found that $\text{G}_{\beta\gamma}$ did not seem to directly interact with the Ca^{2+} channels because NMS-induced I_{Ba} increase was neither accompanied by slow activation kinetics of the I_{Ba} nor removed by a depolarizing pre-pulse. Furthermore, pipette application of peptides which disrupt interactions between $\text{G}_{\beta\gamma}$ subunits and Ca^{2+} channels did not affect NMUR2-mediated I_{Ba} increase. The apparent independence of $\text{G}_{\beta\gamma}$ subunits in the modulation of L-type Ca^{2+} channels may indicate that rat ventricular myocytes express a Ca^{2+} channel that is insensitive to the $\text{G}_{\beta\gamma}$ subunits of G_i -protein binding. An alternative hypothesis is that different Cav1.2 channel splice variants are able to generate different L-type Ca^{2+} channel functions [10]. For example, alternative splicing of the Cav1.2 channel changes the sensitivity of L-type Ca^{2+} channel to dihydropyridines [30]. In addition, it is still possible that NMS-mediated NMUR2 activation does not result in

functionally significant $G_{\beta\gamma}$ activation in adult rat ventricular myocytes.

At present, it is unclear how $G_i\alpha$ -protein increases I_{Ba} . There are several examples of L-type Ca^{2+} channel current modulation by PKA activation [31-33]. For example, L-type Ca^{2+} currents recorded from isolated cardiomyocytes were shown to be increased by glucagon-like peptide-1 via the cAMP-PKA-dependent pathway [34]. By contrast, L-type Ca^{2+} current inhibition by CB1 cannabinoid receptor activation in GT1-7 hypothalamic neurons was prevented by application of PKA inhibitors [35]. Similarly, Cav1.2 current inhibition by integrin receptor activation was blocked by addition of PKA inhibitor H89 [36]. In the present study, we found that the inhibitory effect of NMS on I_{Ba} was independent of PKA, which suggests that some other mechanisms, but not cAMP/PKA pathway, are involved in the stimulatory effect of NMS. Our data showed that PKC- δ was involved in NMS-induced I_{Ba} increase because: 1) pretreatment of cells with classic and novel PKC inhibitors, but not the classic PKC inhibitor, could completely abolish the increase of NMS on I_{Ba} ; 2) the PKC- δ inhibitor rottlerin or intracellular application of a PKC- δ -derived inhibitory peptide, $\delta\text{V1-1}$, but not its inactive analogue abolished the NMS-induced I_{Ba} increase. Our present results were supported by previous studies that activation of novel PKC increases I_{Ba} in neonatal hippocampus [37]. It has also been shown that PKC phosphorylates Cav1.2b $\alpha_1\text{C}$ Ca^{2+} channel subunit, which results in up-regulation of the L-type Ca^{2+} currents [38]. Similar results were reported in rat portal vein myocytes [39]. However, PKC-induced L-type Ca^{2+} current inhibition was also described. For example, in mouse hippocampal neurons, activation of PKC inhibits L-type Ca^{2+} channel currents while an inactive analogue has no effect [26]. This could be explained by a distinct PKC phosphorylation site or different regulation of L-type Ca^{2+} channel subunits ($\text{Ca}_v1.2$ and $\text{Ca}_v1.3$) in different tissues/cell types [33]. An alternative hypothesis is that PKC phosphorylates an intermediate protein that in turn up-regulates the L-type Ca^{2+} channels.

In summary, this study presents a novel action of NMS on L-type Ca^{2+} channel currents in adult rat ventricular myocytes, in which NMUR2, but not NMUR1 was endogenously expressed. NMS significantly increased L-type Ca^{2+} channel currents via stimulation of NMUR2. We provide evidence for a second messenger pathway initiated by NMUR2 that couples sequentially to the $G_i\alpha$ -protein and downstream PKC- δ , which is involved in NMS-induced L-type Ca^{2+} channel stimulation. Whether the same signaling pathway exists in human hearts and the resulting physiological functions requires further investigations in large mammals such as non-human primates.

Acknowledgements

This study was supported by Key Young Project of Shanghai Jiaotong University (to CRX).

Conflict of interest statement

The authors declare that they have no conflict of interests.

References

- 1 Minamino N, Sudoh T, Kangawa K, Matsuo H: Neuromedins: novel smooth-muscle stimulating peptides identified in porcine spinal cord. *Peptides* 1985;6:245-248.
- 2 Brighton PJ, Szekeres PG, Willars GB: Neuromedin U and its receptors: structure, function, and physiological roles. *Pharmacol Rev* 2004;56:231-248.

- 3 Budhiraja S, Chugh A: Neuromedin U: physiology, pharmacology and therapeutic potential. *Fundam Clin Pharmacol* 2009;23:149-157.
- 4 Raddatz R, Wilson AE, Artymyshyn R, Bonini JA, Borowsky B, Boteju LW, Zhou S, Kouranova EV, Nagorny R, Guevarra MS, Dai M, Lerman GS, Vaysse PJ, Branchek TA, Gerald C, Forray C, Adham N: Identification and characterization of two neuromedin U receptors differentially expressed in peripheral tissues and the central nervous system. *J Biol Chem* 2000;275:32452-32459.
- 5 Shan L, Qiao X, Crona JH, Behan J, Wang S, Laz T, Bayne M, Gustafson EL, Monsma Jr FJ, Hedrick JA: Identification of a novel neuromedin U receptor subtype expressed in the central nervous system. *J Biol Chem* 2000;275:39482-39486.
- 6 Mitchell JD, Maguire JJ, Davenport AP: Emerging pharmacology and physiology of neuromedin U and the structurally related peptide neuromedin S. *Br J Pharmacol* 2009;158:87-103.
- 7 Mori K, Miyazato M, Ida T, Murakami N, Serino R, Ueta Y, Kojima M, Kangawa K: Identification of neuromedin S and its possible role in the mammalian circadian oscillator system. *EMBO J* 2005;24:325-335.
- 8 Gardiner SM, Compton AM, Bennett T, Domin J, Bloom SR: Regional hemodynamic effects of neuromedin U in conscious rats. *Am J Physiol* 1990;258:R32-38.
- 9 Singh A, Gebhart M, Fritsch R, Sinnegger-Brauns MJ, Poggiani C, Hoda JC, Engel J, Romanin C, Striessnig J, Koschak A: Modulation of voltage- and Ca^{2+} -dependent gating of Cav1.3 L-type calcium channels by alternative splicing of a C-terminal regulatory domain. *J Biol Chem* 2008;283:20733-20744.
- 10 Zhang HY, Liao P, Wang JJ, Yu de J, Soong TW: Alternative splicing modulates diltiazem sensitivity of cardiac and vascular smooth muscle $\text{Ca(v)}1.2$ calcium channels. *Br J Pharmacol* 2010;160:1631-1640.
- 11 Tang ZZ, Liang MC, Lu S, Yu D, Yu CY, Yue DT, Soong TW: Transcript scanning reveals novel and extensive splice variations in human l-type voltage-gated calcium channel, Cav1.2 $\alpha 1$ subunit. *J Biol Chem* 2004;279:44335-44343.
- 12 Irisawa H, Brown HF, Giles W: Cardiac pacemaking in the sinoatrial node. *Physiol Rev* 1993;73:197-227.
- 13 Bers DM: Calcium cycling and signaling in cardiac myocytes. *Annu Rev Physiol* 2008;70:23-49.
- 14 Benitah JP, Gomez AM, Virsolvy A, Richard S: New perspectives on the key role of calcium in the progression of heart disease. *J Muscle Res Cell Motil* 2003;24:275-283.
- 15 Tao J, Xu H, Yang C, Liu CN, Li S: Effect of urocortin on L-type calcium currents in adult rat ventricular myocytes. *Pharmacol Res* 2004;50:471-476.
- 16 Harmati G, Bányász T, Bárándi L, Szentandrassy N, Horváth B, Szabó G, Szentmiklósi JA, Szénási G, Nánási PP, Magyar J: Effects of beta-adrenoceptor stimulation on delayed rectifier K^+ currents in canine ventricular cardiomyocytes. *Br J Pharmacol* 2011;162:890-896.
- 17 Vainio L, Perjes A, Ryti N, Magga J, Alakoski T, Serpi R, Kaikkonen L, Piihola J, Szokodi I, Ruskoaho H, Kerkelä R: Neuronostatin, a novel peptide encoded by somatostatin gene, regulates cardiac contractile function and cardiomyocyte survival. *J Biol Chem* 2012;287:4572-4580.
- 18 Tao J, Zhang Y, Huang H, Jiang X: Activation of corticotropin-releasing factor 2 receptor inhibits Purkinje neuron P-type calcium currents via $\text{G(o)}\alpha$ -dependent PKC epsilon pathway. *Cell Signal* 2009;21:1436-1443.
- 19 Wang F, Zhang Y, Jiang X, Zhang Y, Zhang L, Gong S, Liu C, Zhou L, Tao J: Neuromedin U inhibits T-type Ca^{2+} channel currents and decreases membrane excitability in small dorsal root ganglia neurons in mice. *Cell Calcium* 2011;49:12-22.
- 20 Zhang Y, Jiang D, Zhang Y, Jiang X, Wang F, Tao J: Neuromedin U type 1 receptor stimulation of A-type K^+ current requires the $\beta\gamma$ subunits of G α -protein, protein kinase A and extracellular signal-regulated kinase 1/2 (ERK1/2) in sensory neurons. *J Biol Chem* 2012; 287:18562-18572.
- 21 Tao J, Hildebrand ME, Liao P, Liang MC, Tan G, Li S, Snutch TP, Soong TW: Activation of corticotropin-releasing factor receptor 1 selectively inhibits Cav3.2 T-type calcium channels. *Mol Pharmacol* 2008;73:1596-1609.
- 22 Blumenstein Y, Kanevsky N, Sahar G, Barzilai R, Ivanina T, Dascal N: A novel long N-terminal isoform of human L-type Ca^{2+} channel is up-regulated by protein kinase C. *J Biol Chem* 2002;277:3419-3423.
- 23 Suzuki T, Seth A, Rao R: Role of phospholipase C γ -induced activation of protein kinase Cepsilon (PKCepsilon) and PKCbeta in epidermal growth factor-mediated protection of tight junctions from acetaldehyde in Caco-2 cell monolayers. *J Biol Chem* 2008;283:3574-3583.
- 24 Belcheva MM, Clark AL, Haas PD, Serna JS, Hahn JW, Kiss A, Coscia CJ: Mu and kappa opioid receptors activate ERK/MAPK via different protein kinase C isoforms and secondary messengers in astrocytes. *J Biol Chem* 2005;280:27662-27669.

- 25 Fenton RA, Shea LG, Doddi C, Dobson JG Jr: Myocardial adenosine A(1)-receptor-mediated adenosine protection involves phospholipase C, PKC-epsilon, and p38 MAPK, but not HSP27. *Am J Physiol Heart Circ Physiol* 2010;298:H1671-1678.
- 26 Zhang Y, Jiang D, Zhang J, Wang F, Jiang X, Tao J: Activation of neuromedin U type 1 receptor inhibits L-type Ca^{2+} channel currents via phosphatidylinositol 3-kinase-dependent protein kinase C epsilon pathway in mouse hippocampal neurons. *Cell Signal* 2010;22:1660-1668.
- 27 Catterall WA: Structure and regulation of voltage-gated Ca^{2+} channels. *Annu Rev Cell Dev Biol* 2000;16:521-555.
- 28 Xu M, Welling A, Paparisto S, Hofmann F, Klugbauer N: Enhanced expression of L-type Cav1.3 calcium channels in murine embryonic hearts from Cav1.2-deficient mice. *J Biol Chem* 2003;278:40837-40841.
- 29 Delmas P, Abogadie FC, Dayrell M, Haley JE, Milligan G, Caulfield MP, Brown DA, Buckley NJ: G-proteins and G-protein subunits mediating cholinergic inhibition of N-type calcium currents in sympathetic neurons. *Eur J Neurosci* 1998;10:1654-1666.
- 30 Liao P, Yu D, Li G, Yong TF, Soon JL, Chua YL, Soong TW: A smooth muscle Cav1.2 calcium channel splice variant underlies hyperpolarized window current and enhanced state-dependent inhibition by nifedipine. *J Biol Chem* 2007;282:35133-35142.
- 31 Martín C, Gómez-Bilbao G, Ostolaza H: Bordetella adenylate cyclase toxin promotes calcium entry into both CD11b+ and CD11b- cells through cAMP-dependent L-type-like calcium channels. *J Biol Chem* 2010;285:357-364.
- 32 Gui P, Wu X, Ling S, Stotz SC, Winkfein RJ, Wilson E, Davis GE, Braun AP, Zamponi GW, Davis MJ: Integrin receptor activation triggers converging regulation of Cav1.2 calcium channels by c-Src and protein kinase A pathways. *J Biol Chem* 2006;281:14015-14025.
- 33 Bünemann M, Gerhardstein BL, Gao T, Hosey MM: Functional regulation of L-type calcium channels via protein kinase A-mediated phosphorylation of the beta(2) subunit. *J Biol Chem* 1999;274:33851-33854.
- 34 Xiao YF, Nikolskaya A, Jaye DA, Sigg DC: Glucagon-like peptide-1 enhances cardiac L-type Ca^{2+} currents via activation of the cAMP-dependent protein kinase A pathway. *Cardiovasc Diabetol* 2011;20:10-16.
- 35 Hoddah H, Marcantoni A, Comunanza V, Carabelli V, Carbone E: L-type channel inhibition by CB1 cannabinoid receptors is mediated by PTX-sensitive G proteins and cAMP/PKA in GT1-7 hypothalamic neurons. *Cell Calcium* 2009;46:303-312.
- 36 Gui P, Wu X, Ling S, Stotz SC, Winkfein RJ, Wilson E, Davis GE, Braun AP, Zamponi GW, Davis MJ: Integrin receptor activation triggers converging regulation of Cav1.2 calcium channels by c-Src and protein kinase A pathways. *J Biol Chem* 2006;281:14015-14025.
- 37 Bray JG, Mynlieff M: Involvement of protein kinase C and protein kinase A in the enhancement of L-type calcium current by GABAB receptor activation in neonatal hippocampus. *Neuroscience* 2011;179:62-72.
- 38 Callaghan B, Koh SD, Keef KD: Muscarinic M2 receptor stimulation of Cav1.2b requires phosphatidylinositol 3-kinase, protein kinase C, and c-Src. *Circ Res* 2004;94:626-633.
- 39 Macrez N, Morel JL, Kalkbrenner F, Viard P, Schultz G, Mironneau J: A $\beta\gamma$ dimer derived from G13 transduces the angiotensin AT1 receptor signal to stimulation of Ca^{2+} channels in rat portal vein myocytes. *J Biol Chem* 1997;272:23180-23185.